Analyst

PAPER

View Article Online
View Journal | View Issue

Cite this: *Analyst*, 2020, **145**, 184

Versatile printed microheaters to enable low-power thermal control in paper diagnostics†

Kristin M. Byers, [a] Li-Kai Lin,[b] Taylor J. Moehling, [a] Lia Stanciu[b] and Jacqueline C. Linnes *[a]

As the capabilities of low-resource field testing have begun to expand to incorporate more complex diagnostic technologies, many of these devices remain tethered to large heaters requiring relatively high-power inputs. Highly efficient microheaters would enable miniaturization of devices for more economic and effective heating with high temperatures and sustained incubation. This work reports the development and application of resistive microheaters printed with nanosilver ink for improved methods of automated sample heating in paper-based point-of-care (POC) and in-field diagnostics. Resistance is easily predicted, and shapes can be altered to fit space and heat-transfer needs, sustained and discrete heating of precise regions are possible. Here, we demonstrate both isothermal nucleic acid amplification at 65 °C and bacterial culture at 37 °C using our microheaters. Printed nanosilver microheaters are easily integrated into reactions that require low-power battery heating, can sustain heating for 16-hour incubations, and cost between 0.17 and 0.58 US dollars each. Further, the microheaters are reusable, stable over 6 months, and can be wetted without degradation or reduction in conductivity. These versatile printed microheaters enable thermal control for a variety of low power heating applications.

Received 12th August 2019,
Accepted 2nd November 2019

DOI: 10.1039/c9an01546a

rsc.li/analyst

Introduction

In-field biological reactions to detect pathogens have been a goal of researchers for many years. A paper-based test was created in 1969 to determine sanitary quality of raw milk by leveraging a color change of resazurin dye induced by the overgrowth of bacteria.[1] More recently, Elavarasan *et al.* and Deiss *et al.* have developed simple plastic and paper-based devices for visual detection of antibiotic susceptibility from cells cultured *in situ*.[2,3] These tests lay the groundwork for in-field bacterial culture devices; however, they still require the use of a commercial incubator at 37 °C for 6 to 18 hours. In contrast, newer isothermal nucleic acid amplification such as isothermal strand displacement amplification (iSDA) and loop mediated isothermal amplification (LAMP) require less than 1 hour of heating but need significantly higher temperatures and/or precise thermal control to produce consistent and sensitive results.[4,5] Thermal management is a critical aspect of these different detection methods.

Advances in microfluidics and electronics have contributed promising devices to attempt to achieve precise, low-power, and sustained heating necessary to implement rapid diagnostic tests at the point-of-care (POC). To date, researchers have used hotplates,[6] custom printed circuit boards (PCBs),[7] coffee mugs,[8] exothermic chemically heated chips and cups,[9–11] thin-film polyimide heaters,[12,13] and traditional incubation ovens[3] as a heat source for POC devices with varying degrees of success.[13,14] Standard laboratory-grade incubation ovens are accurate and can incubate large volumes of samples at one time, however even a 'mini' six liter incubator requires 80 watts of consistent power that can only be obtained from a modern electrical grid or a generator.[15] Although chemical heaters do not require batteries or external power supplies, they typically rely on highly variable exothermic reactions such as magnesium iron alloy (MgFe) and saline cartridges which are single-use and are difficult to control without a phase change material (PCM) chamber to buffer the sample temperatures.[10,16–18] Current PCB-based heaters, while effective, require long copper traces which result in slow ramp-ups to the target temperature and excess heat and power consumption.[7] In Hwang *et al.*, sample overheating and control of the working voltage for each heating stage of a polymerase chain reaction (PCR) to detect *Chlamydia trachomatis* remained problematic even after reducing the size of the heating pattern and utilizing a complex electronics system to perform the thermocycling.[19] Large thin-film polyimide heaters present similar overheating and power consumption issues but could be useful if successfully miniaturized. Hot plates and coffee mug-

[a]*Weldon School of Biomedical Engineering, Purdue University, West Lafayette, IN, USA. E-mail: jlinnes@purdue.edu*
[b]*School of Materials Engineering, Purdue University, West Lafayette, IN, USA*
†Electronic supplementary information (ESI) available. See DOI: 10.1039/c9an01546a

based units are also oversized and require excess energy to heat the enclosed space. In order to effectively implement POC and in-field diagnostics in low resource settings, there is a critical need to continue improving these technologies for integration of custom, well controlled, localized heating of reactions and other components either into the disposable device itself or into a supporting reusable electronic platform.

Printed microheaters have shown promising and predictable heat transfer properties.[20–22] These printed heaters rely on joule heating (also referred to as resistive/ohmic heating) wherein the energy of an electric current is converted into heat as it flows through a conductive material of known resistivity.[20] Many materials-based publications have demonstrated that ink-jet printed silver traces providing conductive lines on various substrates can be fabricated with acceptable consistency, conductivity, and mass-produced *via* roll-to-roll manufacturing.[23–25] These traces can be customized by varying the number of printed layers[26] and sintering treatments to increase conductivity. Sintering and curing techniques commonly used for printed conductive traces are electrical sintering,[27] heat annealing/baking,[28] lasers,[29] and intense pulsed light.[30] Substrates including photo paper,[28] chromatography paper,[31] PET,[20,28] glass,[32] and other custom films have all been used for biosensing electrodes[31] and even capacitors for integrated circuits.[33] The thermal properties and conductivity of traces using other materials including copper and carbon in roll-to-roll manufacturing have also been investigated.[25,34] These research efforts present a number of promising conductive traces. By leveraging the precision and scalability of printed microheaters, we have developed versatile, robust, and sustained heating for various biological reactions.

Our low-cost, low-power, inkjet-printed resistive microheaters have been uniquely designed to provide rapid and sustained low-power thermal control of biological reactions at localized regions in paper-based assays. By changing the inherent resistance of the trace using different serpentine designs and printing settings, we can precisely control local temperatures during incubation of biological samples for prolonged periods of time, enabling reactions that vary from 30-minute LAMP at 65 °C to 16-hour bacterial culture at 37 °C. The microheaters are robust enough to be re-used for many months, yet low cost enough for disposable assays. The microheaters can be integrated into diverse platforms using an variety of power sources.

Experimental methods

Reagents and materials

Microheater materials included Nanosilver Ink (JS-B40G, Novacentrix Austin, TX), Kapton substrate (Kapton HN Semi-Clear Amber film, 5 mil 125 μm, DuPont, Circleville, OH), and Kapton tape (3M 5413 Dupont, DuPont, Circleville, OH). Power sources included a 1550 DC power supply (BK Precision, Yorba Linda, CA), and a rechargeable AA 2600 mAh (1.2 V NiMH, Tenergy, Fremont, CA).

Escherichia coli (*E. coli*) strain C2987 (New England Biolabs, Ipswich, MA) grown in LB growth media (L3022 Millipore Sigma, Darmstadt, Germany), 10X PrestoBlue™ (Life Technologies Corporation, Carlsbad, CA) used for detection of cellular growth. Paper chip materials include G041 Glass Fiber pads (GFCP103000, Merck Millipore, Darmstadt, Germany), and clear adhesive laminating sheets (#3747307, Swingline, ACCO Brands, Booneville, MS).

Vibrio cholerae (*V. cholerae*) strain N16961, a toxigenic O1 serogroup, was provided by Dr Afsar Ali, from the Department of Environmental and Global Health at the University of Florida. LAMP assay reagents included six primers detailed in Table S1† (Integrated DNA Technologies, Skokie, IL), *Bst* 2.0 polymerase (NEB, Ipswich, MA), deoxynucleotide triphosphates (dNTPs) (Agilent Technologies, Santa Clara, CA), isothermal buffer (NEB, Ipswich, MA), betaine (Millipore Sigma, Burlington, MA), EvaGreen (VWR International, Radnor, PA), ROX (Thermo Fisher Scientific, Waltham, MA), molecular biology water (Invitrogen, Carlsbad, CA). Paper chip materials include: polyether sulfone (PES) samples with 0.22 μm pores (SLGP033NS, MilliporeSigma, Burlington, MA), polyethylene terephthalate (PET) film (Apollo, Lake Zurich, IL), clear adhesive laminating sheets (#3747307, Swingline, ACCO Brands, Booneville, MS).

Inkjet printing method

The resistive microheaters were printed using a Dimatix printer (DMP-2850, Fujifilm North America Corporation Valhalla, NY) which uses piezoelectric inkjet technology to deposit path designs (traces). Nanosilver Ink containing 40% silver by weight was applied by the Dimatix onto a Kapton substrate. The Nanosilver ink was filtered through 0.2 μm filter (Whatman® Puradisc 13 syringe filters made of 0.2 μm, PTFE,) to remove large aggregates. Print settings included 35 μm drop spacing at room temperature with platen vacuum on and platen temperature set to 50 °C. The waveform file directing recommended jetting voltages was provided by Novacentrix Inc. Designs were created in Adobe Illustrator (Adobe Systems Incorporated, San Jose, CA) with variable path lengths, line widths, and cross-sectional areas (summary of designs in Fig. S1†). The printed traces were heat cured *via* baking at 400 °C for 10 min. These printing and curing methods were used for all heating characterization and application studies.

Microheater characterization

Individual traces were measured post-curing with a handheld multimeter (AM-510, Amprobe, Everett, WA) to determine initial resistance and re-measured before each use. The resistance of printed lines was determined by the two-point probe method. These measurements were then compared with predicted resistance calculations based on path length *versus* cross sectional width ratio as it relates to overall microheater resistance (Table S2†).

Scanning electron microscopy (SEM)

A FEI NOVA nanoSEM field emission SEM was used with a Through-the-lens detector (TLD) for high magnification (50 000×) with 4.6 mm WD, 10 kV, 6.00 μHFW and 3.0 spot size. Cured samples were imaged with and without a sputtered layer of platinum.

Profilometry

A KLA-Tencor, model P-7 stylus profilometer (KLA Corporation, Milpitas, California) was used with 65 μm/0.0391 Å resolution, 0.50 mg applied force, 100 μm s^{-1} scan speed, and varying scan sizes between 8000 and 10 000 μm for designs of differing trace widths, between different print jobs, and in different locations of the printed traces.

Heating evaluations

An infrared (IR) thermal imaging camera (A300 Series, FLIR Systems, Sweden) and a 1550 DC Power Supply (BK Precision, Yorba Linda, CA) were used to characterize the initial and long-term heating of the microheaters. The initial characterizations with non-insulated samples provided initial power settings which were then adjusted for sample needs (specified in later sections). A heating consistency test was done to assess reusability. A 5 Ohm microheater (design 1_1) was heated 10 times for 15–20 minutes each using 220 mW DC power each time while a K-type temperature sensor read by an RDXL4SD Thermometer (Omega Engineering Inc., Norwalk, CT) was taped to the top edge of the center of the microheater which was then covered with Styrofoam and enclosed in the plastic box. When paper chip-based samples were introduced for *E. coli* and *V. cholerae* LAMP incubations, the thermocouples were taped to the top and bottom edges of the samples to more accurately assess the sample temperature.

Durability testing

A representative sample of design A (1.8 cm in total length) was used to perform a simplified test similar to Cordill *et al.*'s methods[35] for strain testing of thin films on polymer substrates. This included first measuring the initial total length (L_0) of the sample and initial resistance (R_1) of the trace using the two-point probe method with a multimeter (AM-510, Amprobe, Everett, WA). The sample was then subjected to bending between two gloved fingertips in both the convex and concave conformations at which point the change in length (ΔL) was manually measured and recorded. The resistance of the sample was again measured (R_2) and the change in resistance ($\Delta R = R_1 - R_2$) and strain ($\varepsilon = \Delta L/L_0$) were calculated. Another representative sample of design A was placed in distilled water for 3 days with pre- and post-treatment resistance measurements recorded with the two-point probe method. Another series of tests were performed on design 1_1.

E. coli incubation and detection methods

E. coli samples were grown in LB in an incubator shaker at 200 rpm at 37 °C overnight. Cultures were diluted in LB media to an OD_{600} of 1, (Ultrospec 10, Biochrom, Cambourne, UK) representing 8×10^8 cells per mL of *E. coli* as determined by counting colony forming units of serially diluted samples. 5 μL of 10X PrestoBlue™ was added to 45 μL samples of serial dilutions of *E. coli* in LB. 50 μL samples were placed on 10 × 10 mm glass fiber pads and the devices were sealed with 25 × 25 mm clear adhesive laminating sheets. One set of dilutions was kept at room temperature (protected from light exposure) and another placed in a microbiology incubator at 37 °C. Negative controls containing 45 μL of LB and 5 μL PrestoBlue™ were included in each batch.

A 10^4 colony-forming unit (CFU) per mL sample was prepared as above (final concentration 9 CFU μL^{-1}) and individually incubated with our "design A" microheater (Fig. 1B) heated by the 1550 DC power supply for 16 hours (two identical controls were also placed in the lab-grade incubator and left covered at room temperature. Two K-type temperature sensors read by were placed on the top and bottom faces of the sample chip and covered with tape to provide better sampling of the paper chip temperature. In an opaque box, a battery and glass slide were secured and the Styrofoam insulation for the sample was cut to match the size of our incubation chips which was taped down (schematic shown in Fig. 1C).

An additional test was done with a 10^6 CFU mL^{-1} sample of *E. coli* prepared as above (final concentration 900 CFU μL^{-1}). A single rechargeable AA battery (AA 2600 mA h 1.2 V NiMH) powered the microheater setup inside an opaque plastic container for 6 hours. This higher concentration was used for simplicity of the repeat and is comparable to other publications showing proof-of-concept detection with resazurin.[3] Following incubation, all samples were scanned with an Epson V850 Pro Scanner (Model J221B, Epson America Inc., Long Beach, CA) with the same scan settings. The Red and Blue channel average intensity color values of all samples were measured using a MATLAB script[36] which were then used to calculate the ΔRedBlue (ΔRB) value detailed in eqn (1). These values were then graphed and compared.

$$\Delta RB = \sqrt{(R_1 - R_2)^2 + (B_1 - B_2)^2} \quad (1)$$

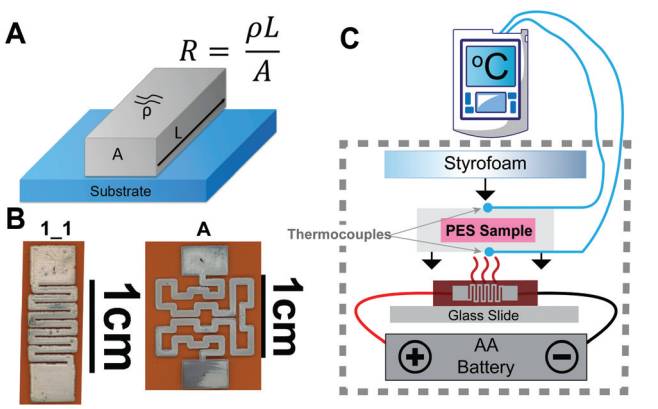

Fig. 1 (A) Resistivity of a conductive trace schematic. (B) Two representative designs (1_1 and A) used in experiments. (C) Schematic of experimental setup for battery powered incubations.

Nucleic acid amplification in paper methods

V. cholerae cultures were grown in LB media overnight at 37 °C using a miniature incubating shaker at 300 rpm (Thermo Fisher, Waltham, MA). Cultures were diluted in LB media to an OD_{600} of 1, (Ultrospec 10, Biochrom, Cambourne, UK) representing 6×10^8 cells per mL of *V. cholerae* as determined by counting colony forming units of serially diluted samples. LAMP was performed to amplify DNA from *V. cholerae* at a concentration of 4×10^5 cells per mL ($\sim 10^4$ cells per reaction, where 1 reaction is 25 μL). LAMP samples were incubated in 7 mm × 7 mm PES membranes with 0.22 μm pores, covered on both sides with 10 mm × 10 mm PET film, and sealed with 15 mm × 15 mm adhesive laminating sheets to prevent evaporation during heating. The no template negative control consisted of molecular biology grade water rather than template (Thermo Fisher Scientific, Waltham, MA). All samples were incubated at 65 °C on top of a single resistive microheater (design 1_1) and insulated with a thin Styrofoam square for the 30-minute amplification assay (Fig. S2†). The entire circuit and sample was enclosed in a plastic box to limit heat loss *via* convection. Positive and negative samples were amplified in an Applied Biosystems 7500 Real-Time PCR System (Foster City, CA) for 30 minutes at 65 °C as gold standard heating controls. The negative sample was incubated the same way as the positive samples but was done separately to avoid contamination. Power was supplied to the microheater *via* a freshly charged battery (AA 2600 mA h 1.2 V NiMH, Tenergy, Fremont, CA). This same battery was used for subsequent heating sessions, providing power for four ~30-minute heating sessions.

The temperature of the sample was monitored for the entirety of the assay to ensure that the sample remained in the temperature range of 60–70 °C in which the *Bst* 2.0 polymerase has 100% activity.[37] Two K-type temperature sensors read by an RDXL4SD Thermometer (Omega Engineering Inc., Norwalk, CT) were placed on the top and bottom faces of the sample chip. Each LAMP reaction was heated for 30 minutes, starting when the bottom face of the sample chip reached 65 °C, and was continuously monitored for overheating. The microheater was in use for approximately 35 minutes for each session. The PES membranes were place in microfuge tubes and centrifuged at 2.0 rpm for 60 seconds to release the amplicons from the PES membrane. After centrifugation, 5 μL of amplicons were added to a commercial lateral flow immunoassay (LFIA) (Ustar Biotechnologies, Hangzhou, China) for analysis. The LFIAs were scanned at least 30 minutes after initial sample addition using an Epson V850 Pro Scanner. The test band was quantified using a custom MATLAB script that averages the grey-scale pixel intensity of the test band and subtracts the average background pixel intensity 25 pixels below the test band.[36]

Statistical analysis

Means and standard deviations of the resistances of each printed trace design were compared with a minimum of 25 prints for each design. The few microheaters that were not conductive or were visibly deformed or nonfunctional were excluded from these results so as not to skew the mean batch resistance. A one-way ANOVA and multiple comparisons test (Tukey) were performed in GraphPad on the single resistor reusability test data.

COMSOL modeling

In order to confirm our temperature sampling methods during the pathogen detection experiments and further characterize the heating distribution throughout samples heated by the different microheater designs, we created a physics-based software model. Evaluations of the heating profiles produced by the microheaters (through the sample chips) were performed in COMSOL (Multiphysics v5.4, COMSOL Inc., Burlington, MA) using the Heat Transfer and AC/DC Module licenses. These models were built based on the early characterization and experimental IR imaging data. A convective heat flux with ambient air (20 °C) was the primary source of heat loss on the external surface of the sample and heater assembly. Radiation Effects were not included in the final model as they were found to be negligible. Using experimental data of the sheet resistance resulting from the printing/sintering methods and known parameters of other materials, a simple model was used to confirm and estimate heating of the microheater/sample experiments performed in this paper. A solid pyramid was used to simplify the many portions of the paper chip and conform to the approximate shape of the paper and plastic chips used in experiments to contain samples. A volume of water was placed inside the pyramid to represent the true samples in experiments. Measurements of size and thickness were estimated for some materials used in the model (details in Table S3†) but every effort was made to match real materials used. Temperature-dependent resistance changes were not modeled because no resistance changes were measured during heating to relevant temperatures in experiments. The model designates the conductive trace as a surface element and uses a "shells" method to define the conductivity of the trace based on inputs of conductivity and thickness – both of which had been previously measured during characterization. Designs were imported from their original Illustrator design files into COMSOL.

Results and discussion

Heating design and theory

Resistive heating is the process where the energy of an electric current is converted into heat as it flows through a material of known resistivity (ρ).[20] By changing the inherent resistance of the conductive printed trace by using different serpentine designs, we were able to control the amount of heat-energy that is produced by the trace in a given area. The overall resistance of the trace is determined by calculating the area of the perpendicular face of the trace and the path length of the trace (represented by eqn (2)).

$$R = \rho \frac{L}{A} \tag{2}$$

where R is measured resistance (Ohms) of the printed trace, ρ is resistivity, A is cross-sectional area (m^2) and L is the length (m) of the printed trace.[38] This was used to estimate the resistivity of the cured ink with an estimated z height of printed material for a single layer of 40% nanosilver ink being between 0.5–1 μm from profilometry readings detailed in Fig. S3.† The profilometry data also revealed considerable variation in z height. Because this data was acquired on a flexible substrate that may warp under pressure of the profilometer, some of the data may be skewed for this reason. The profilometry sensitivity, while more accurate than any other measurement technique, may in fact exaggerate the topography roughness. Regardless, we cannot assume a perfectly flat trace due to drop spacing, drop overlap, print head clogging and other variant factors inherent to the printing process. One clear conclusion from this investigation is that the width of the printed trace and the drop spacing settings must be optimized for very thin traces (less than 0.1 mm) as thinner traces tend to have a larger z height due to surface tension interactions.[39]

The profilometry revealed inconsistencies in printed z height between designs of varying trace thicknesses (width). Specifically, design 1_1 with 0.53 mm width had a z height of 600–800 nm (Fig. S3†) while design 1_2 (Fig. S1†) with 0.35 mm width had an average z height of 1000 nm. This suggests that if one desires a more consistent z-height across a trace, the designed width/thickness should not be less than 10× the set drop-spacing and care should be taken to ensure the optimum number of print heads are activated and not clogged. The effect of drop spacing on inkjet-printed thickness has been investigated previously and largely depends on the viscosity and surface tension properties of the ink and substrate interactions.[40] The Novacentrix ink we used is water based and has a viscosity of 8–12 cP with a surface tension of 28–32 mN m^{-1}. The Kapton substrate surface energy is also 28–32 mN m^{-1} and was chosen after testing several other substrates including HP Photopaper (glossy), Novele™ substrate (from NovaCentrix), and others. The profilometry data allowed us to gather an average z height of the traces to predict the resistance of new designs. These calculations are detailed in Table S1.† The first set of designs were averaged and an average resistivity from each batch was calculated and compared. The general resistivity of the printed traces resulting from these methods is 43.0 μΩ mm. This converts to 2.3×10^7 S m^{-1}, while bulk silver has electrical conductivity of 6.16×10^7 S m^{-1}. It is expected that bulk silver would be more conductive than the printed traces, which are known to have surface defects and printing inconsistencies. After this, we used the resistivity to quickly calculate a predicted resistance of an entirely new set of traces (design A, B, C, D with heating regions 11.9 × 9.2 mm to 23.7 × 18.3 mm, Table S2, Fig. S1†).

Printed microheater characterization and design analysis

From SEM images of the fabrication results (shown in Fig. 2), it is clear that the Kapton substrate and silver ink with baking resulted in a semisolid layer of conductive bulk silver when compared to literature.[28,38] This curing method simply involves the evaporation of solvent leaving the remaining 40% bulk silver on the surface of the substrate.[38] A curing treatment protocol by Shen *et al.* with 25 wt% nanosilver ink produced a semi solid layer similar to ours but with more gaps between particles and smaller coalesced grains.[28] Although average particle size in the liquid ink is 60–80 nm,[41] the curing process clearly resulted in nanoparticle coalescence creating a semisolid film. Grain formation appears to have occurred with average grain size being 250–500 nm and larger aggregates up to 800 nm to 1 μm in diameter. This grain formation is a well-known phenomenon and previous microstructural characterization has revealed differences in conductivity for small *versus* large grains.[38] Results by Saraf *et al.*[42] showed an increase in conductivity for higher curing temperatures compared to lower temperatures for microparticle based inks. Additionally, the depression of melting temperature for silver nanoparticles, known as the "scaling law",[43] is well documented in nanoscale literature. Surface defects such as small gaps between grains are common for these methods but are not of great concern for the application of heating. Additional thermal IR imaging showed no hot spots on any printed microheaters, indicating consistent heating ability along the printed traces. The high conductivity, simple production process, and consistent heating qualifies these traces as functional for the purpose of heating small samples.

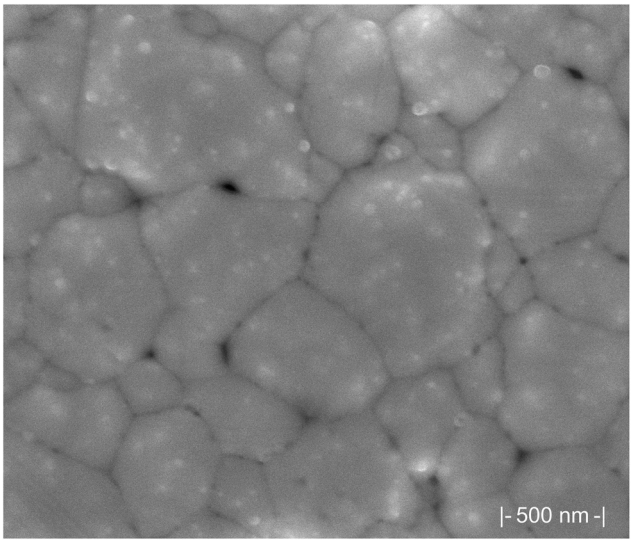

Fig. 2 SEM of printed trace on Kapton film, post-curing showing a semi-solid layer of highly coalesced nanoparticles forming large grains suggesting high conductivity.

By maintaining a single print layer, we were able to optimize the width of the printed design and the path length of the trace for each heating area. Although there are slight differences between individual microheater resistances, these differences are incurred by the printing process and do not greatly affect the functioning of the microheaters, nor does it drastically affect the power consumption. Having characterized the simple serpentine designs (Fig. S1.† designs 1_1, 2_1, 1_2, 2_2, 1_3) and verified an acceptable resistance estimation

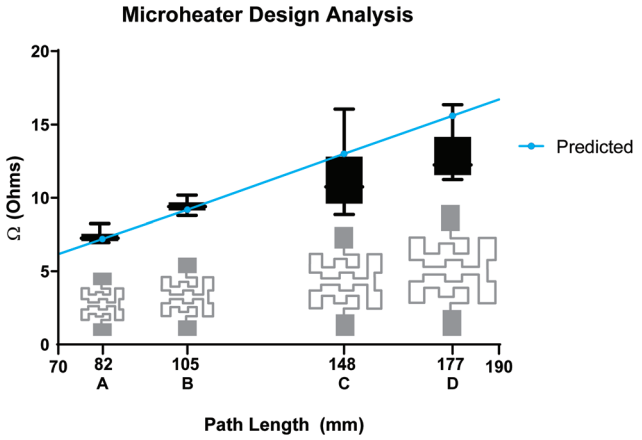

Fig. 3 Analysis of printing results comparing printed *versus* predicted resistance of new microheater designs. Design shapes in grey. As path length increases, resistance of the traces increases also increases proportionately. Box plots of printed resistances (n = 25, N = 4 batches) in black with error bars representing max and min values. Predicted resistances shown in blue are 7.2, 9.2, 13.0 and 15.6 Ohms and average printed resistances were 7.4, 9.5, 12, and 15.3 Ohms for designs A, B, C, D respectively. This prediction method was accurate within 1 Ohm for larger print designs when printed in 4 batches of 25 microheaters per design.

method based on the properties defined in Table S2,† we were able to quickly move to more complex designs (Fig. 3. A, B, C, D) covering a larger area by applying eqn (2). Our predicted resistances of the printed traces closely matched the final average resistance of each design. Some deviation from estimated resistance was expected due to the variation induced by the printing and sintering processes, however we were able to predict the resistance of a trace within 20% of the average for all traces. Average resistances of printed microheaters were all less than the predicted resistance. We assumed an average z height of 700 nm for remaining designs A, B, C, and D, which proved accurate for design A, which had a z-height of ~700 nm (Fig. S3†). Despite each of these designs being set at the same path width (0.7 mm), the predicted results (blue line shown in Fig. 3) were less accurate than anticipated for the larger designs (C and D). This is likely due to a slight difference in z height of the printed layer (as seen in the profilometry data in Fig. S3†) or in varying coalescence of silver nanoparticles between different batches. Despite these variations, this predictive method is useful as a guideline for new designs until measurements from a large batch of printed microheaters can be made. It may be worthwhile to simply make predictions of maximum and minimum expected resistances based on a given design by using the minimum and maximum expected z heights resulting from a single layer of the inkjet-printed ink. Any resulting traces above these maximum values would suggest a clogged print head, poorly mixed ink, or unsuccessful curing. Traces below estimated resistance values benefit from the particle coalescence discussed previously. The print analysis for designs C and D in Fig. 3 suggest that the variability of the measured resistances may seem to scale with the size of the traces. However, more investigation with different designs would be needed to properly assess this phenomenon and rule out simple printing process issues such as a clogged or mis-firing print head. Ultimately printing variability issues with respect to microheater size and design would change in the event of scale-up production *via* roll-to-roll printing and optimization of that process has been as source of many other investigations.[23] This suggests that scaled-up production of these microheaters could be possible and the prediction of certain microheater designs *via* eqn (2) could aid in the optimization of that printing process as well as in the creation of new designs for more uses than we present in this paper. In fact, linewidths of 1 μm have been shown to be achievable with a combination of certain roll-to-roll and inkjet printing methods with silver ink.[44] Meanwhile, a more traditional roll-to-roll system reached a linewidth of 20 μm by adjusting the force applied between the rollers involved in ink application.[45]

We characterized the IR heating profiles for each power input in relation to overall microheater performance of the two microheater designs used in subsequent application-based experiments (Fig. S4†). Fig. 4(A & C) shows the average temperature over the designed heating region over time for each power input. Fig. 4(B & D) shows representative IR profiles of the 0.8 V input, which reveal an even heating profile along the printed traces without hotspots suggesting that a sample in contact with this microheater would experience a diffused but even heating. The average temperature of the rectangular heating region (outlined in blue in Fig. 4B & D) has an average temperature of 62.7 °C (max 67.2 °C, min 53.0, STD 3.27) for B and an average temperature of 42.0 °C (max 49.1 °C, min 34.5 °C, STD 3.21) for D. Because of heat dissipation through the Kapton film which has a coefficient of thermal conductivity of (0.12 W m^{-1} K^{-1})[46] and heat transfer into varying sample sizes, higher power settings may be required for a sample to reach the same temperatures shown in the IR thermal analysis. These results represent the minimum power requirements for a given microheater design to reach each temperature. Based on these results, a design 1_1 microheater with a resistance of about 5 Ohms can successfully heat a LAMP reaction using only 0.8–1.2 V when considering heat dissipation into the sample.

No resistance drift was observed during IR heating tests, which was indicated by no change in current draw from the initial contact with the power source during heating. Because there is no resistance drift for these resistors, we can easily maintain both temperature and power settings. Pardy *et al.* evaluated commercial prototype elements and maintained temperature between 60–63 °C for 25 minutes[47] featuring heating elements that increase in resistance with temperature. They claimed this resistance drift made the heaters self-regulating. However, this function may not be reliable in environmental conditions found in the field or in low resource POC settings if ambient temperature shifts are large. Additionally, our results show that for different voltage inputs (0.6 to 1.0 volts) lower resistance microheaters produce a wider range of temperatures compared to higher resistance microheaters (Fig. 4A and C). This voltage sensitivity at lower resistances

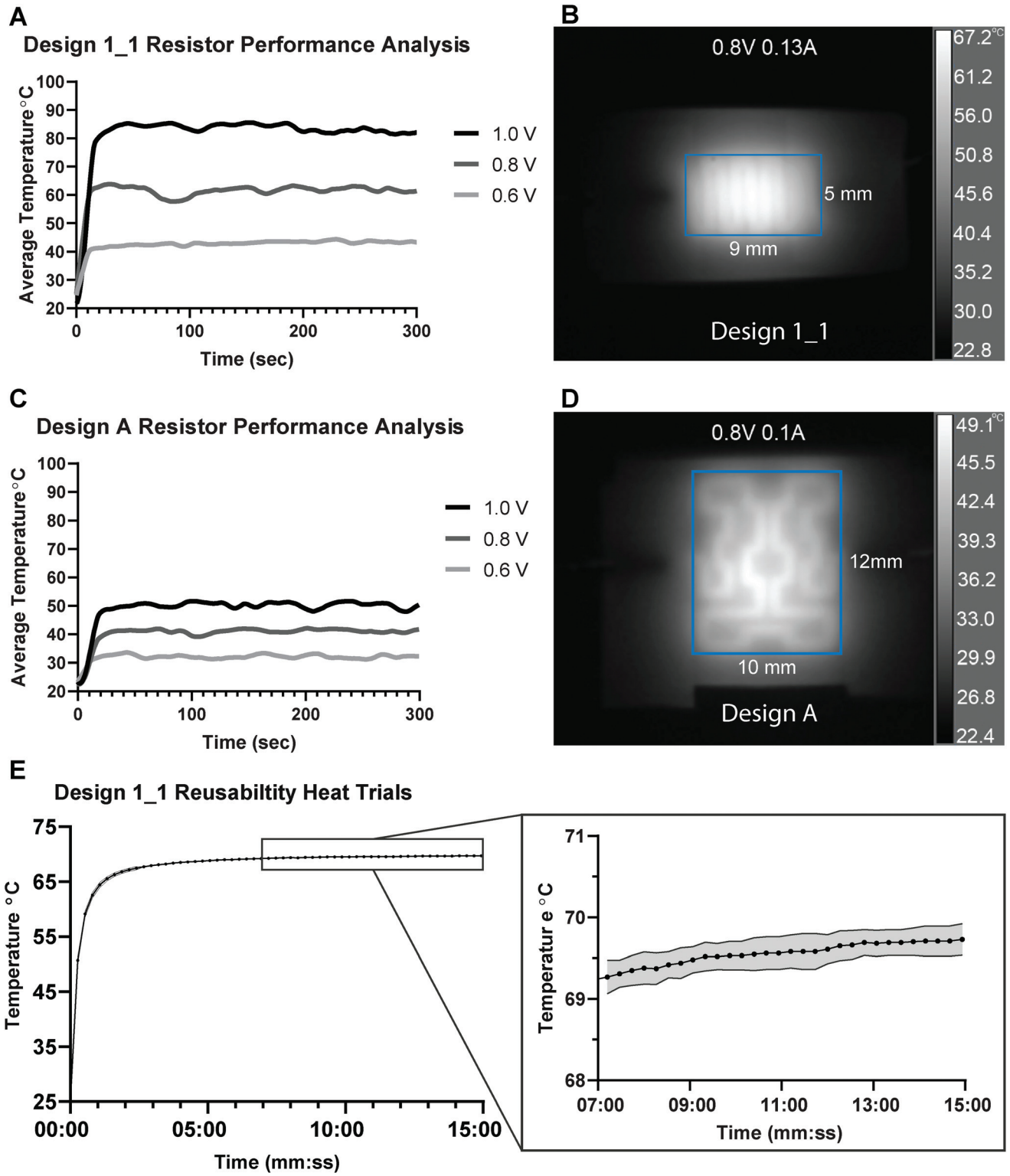

Fig. 4 Analysis of individual microheaters design 1_1 (5 Ohms) and design A (8 Ohms). (A & C) Microheater temperatures over time at various voltage inputs (averaged over square heating area outlined in blue in IR images to right). (B & D) IR images of microheaters at 300 seconds of heating with higher temperatures represented as lighter and lower temperatures represented as darker greyscale intensities. (E) Average of 10 trials of repeated heating of a single 5.5 Ohm microheater from design 1_1 (left) and detailed view (right) grey shaded region represents variability (standard deviation).

could be exacerbated by heaters with initial resistances less than 5 Ohms which would increase initial heating inconsistencies. The "self-regulating" heaters had average initial resistances of 0.8 Ohms and average steady-state resistance (heated-up) of 13.6 Ohms which ultimately required 3 V of DC power to reach 61.5–64 °C.[47] In our work, a single 5.5 Ohm microheater was heated for 15 minutes for ten trials and produced heat curves with no significant difference between heating trials and standard deviations between 4.3 and 4.9 within the trials (Fig. 4E, Tables S4 and S5†). This microheater was able to repeatedly reach 65 °C within 1 minute of initiation and maintain 65–70 °C using constant power settings of only 220 mW (1.1 V, 200 mA). These results show that the microheaters are highly consistent between heating trials and are reusable with no resistance shift resulting from the microheaters being heated.

Additional evaluations were performed in COMSOL to test the heating profiles and heat transfer produced by the micro-

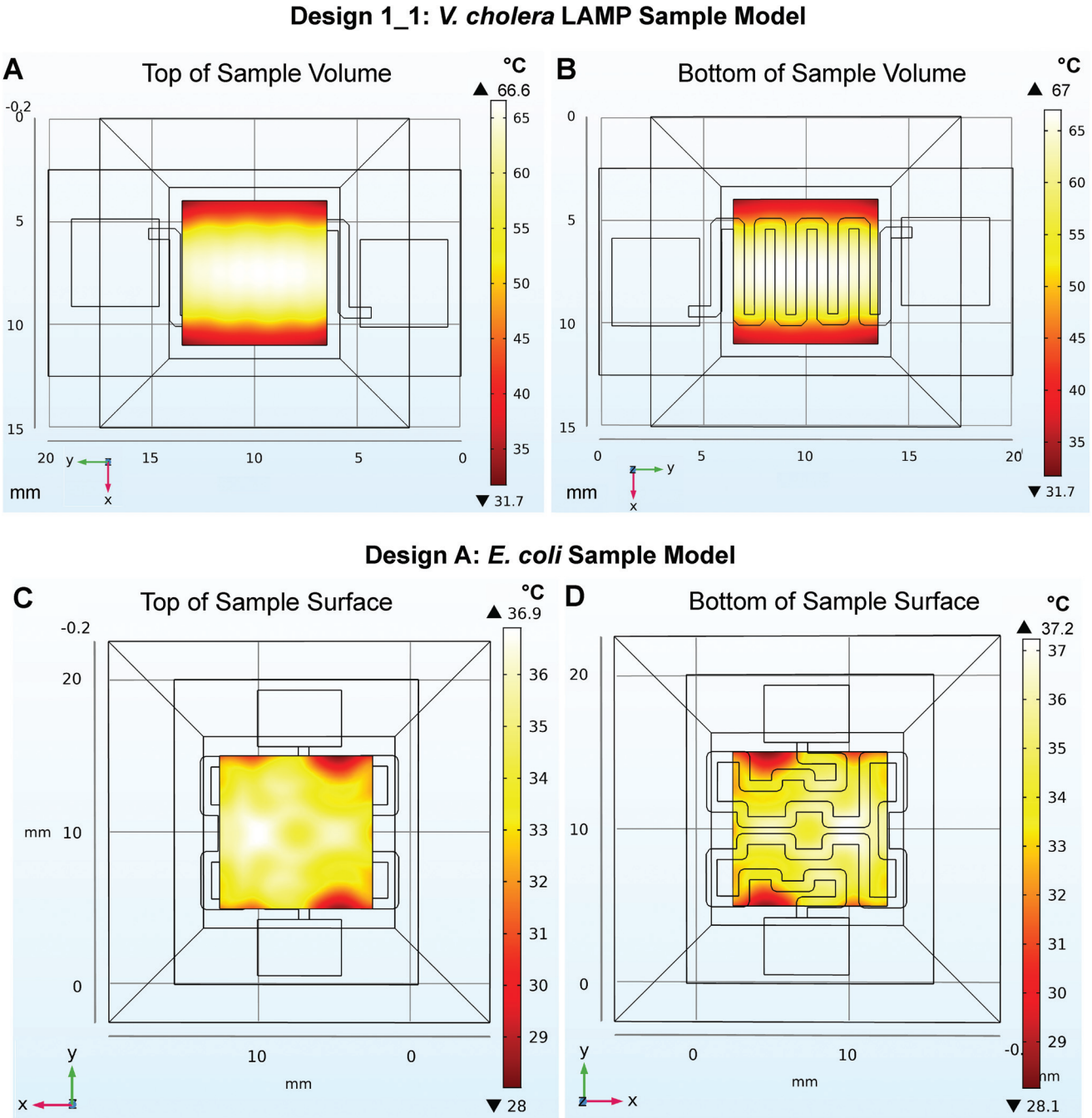

Fig. 5 COMSOL model results of liquid sample temperature distributions. A and B represent the top and bottom of the sample heated by design 1_1 in the *V. cholera* LAMP experiments while C and D represent design A heating the *E. coli* sample.

heaters through the sample chips used in the experiments below. These models demonstrate the range of temperatures produced within the liquid samples using microheater designs 1_1 and A as shown in Fig. 5 below. In design 1_1, the temperature of the surface of the microheater ranges from 20 °C to 76.2 °C, the surface of the sample chip in contact with the microheater ranges from 20 °C to 71.2 °C, the liquid sample at the center of the chip is from 31.7 °C to 67 °C, with an average volume temperature of 63 °C. In design A, the temperature of the microheater surface is 20 °C to 43 °C, the surface of the sample chip in contact with the microheater is 20 °C to 40.6, the liquid sample at the center of the chip is 28.1 °C to 37.2 °C, with an average volume temperature of 35 °C. Additional model outputs showing these results are presented in Fig. S5 and S6† along with model parameters in Table S3.† This computational investigation was a valuable tool that showed design A produced a much less consistent heating area than design 1_1. While this reduction in uniformity was expected given the larger spacing between the traces, the extent to which the model showed this could affect the sample was more extreme than anticipated. This model could be useful for evaluating future designs prior to the printing stage, especially when testing trade-offs between low-resistance designs and large surface area needs. The model does not address heat build-up that may have occurred in the enclosed case used in later experiments. However, during experiments there was imperfect contact between the sample chip and the microheaters due to thermistors used to record temperatures on the top and bottom of the sample chip. With all limitations considered this model is a good representative of best-case heat transfer between the microheater and sample chip.

Durability and cost analysis

The microheaters were found to have only a 0.1 Ohm (or 1.3 percent) change in resistance and did not retain any visible deformation after being subjected to both concave and convex bending, resulting in a strain of $\varepsilon = 0.16$ for a design A microheater covered in Kapton tape (Fig. S7A†). A series of more aggressive bending on a single design 1_1 microheater (covered in Kapton tape) showed excellent durability despite creasing of the Kapton substrate (Fig. S7B†). After this creasing in one direction, the change in resistance was 0.2 Ohms. Creasing in the other direction resulted in an additional 0.3 Ohm increase. This aggressive treatment resulted in a total resistance change of only 0.5 Ohms (9.3 percent difference) and did not otherwise affect the performance of the microheater. Although these microheaters are not intended for use on the skin like Sadri *et al.*'s larger epidermal heaters,[49] the flexibility and durability of this substrate and ink combination provides robustness when heating regions within in-field or POC diagnostics. The microheaters can withstand submersion in distilled water for 3 days without measurable change in resistance, indicating these microheaters are compatible with wet samples and can be used in the field. Further, the microheaters maintain a stable resistance over a three-month time period at room temperature. By covering the printed traces with Kapton tape or storing the microheaters in an oxygen reduced environment, we can halt resistance changes due to oxidation of silver nanosurfaces. When covered with Kapton tape the microheater resistances remain stable over 6 months and could likely remain stable for much longer. The cost of the printed microheaters is significantly less than that of commercial thin-film heaters. The smallest commercial polyimide heaters available from Omega are 1 × 1 inches and are sold for ~$52 each. Meanwhile, our microheaters have an estimated material cost of $0.17 for design 1_1 and $0.58 for design D which was the largest design printed (Table S6†) and can be designed to reach resistances as low as 2 Ohms (Fig. S8†). We have summarized these, and other factors to examine when

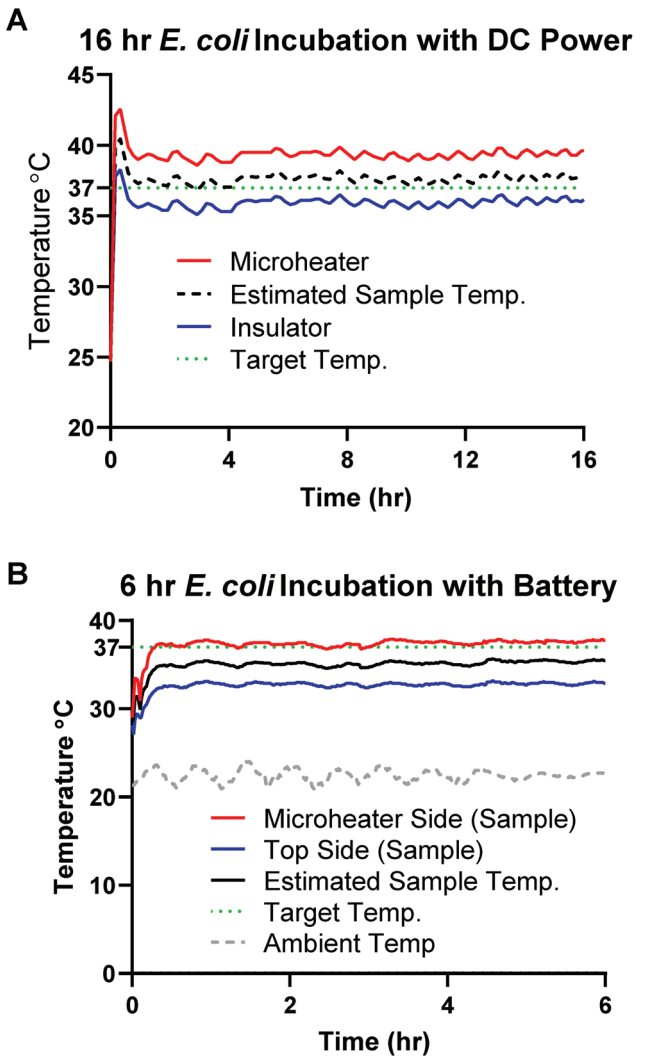

Fig. 6 *E. coli* microheater incubations. (A) 16-hour constant incubation of *E. coli* with 1550 DC power supply and 8.5 Ohm microheater. The power settings were initially set to 143 mW and then was reduced to 120 mW and maintained for the entire 16 hours, using ~1920 mW h (milliwatt hours) for the entire incubation. (B) The *E. coli* incubation was successfully heated with design A (8 Ohms) powered by a single rechargeable NiMH AA battery supplying an average current of 145 mA (1.2 V, power ~174 mW), using an estimated 1044 mW h (milliwatt hours) for the 6-hour incubation period.

considering suitability of heating methods for POC diagnostics in Table S7.†

Application-driven heating

Incubation and detection of *E. coli via* resazurin colorimetric growth assay. During cell growth, *E. coli* produce nicotinamide adenine dinucleotide (NADH). NADH catalyzes the reduction of resazurin (the active compound in PrestoBlue™) to resorufin, resulting in an easily identifiable color shift from blue to pink.[50] This well-known phenomenon was used to indicate and assess the incubation of *E. coli* in trials of DC and battery-powered incubations with microheater design A. No resistance drift was observed for the entirety of the 16-hour incubation, indicated by the consistent current given by the DC power source. Fig. 6A shows the consistent temperature profile which also demonstrates that the sample reached 37 °C within 10 minutes of initiation. Based on this experiment, it was estimated a single rechargeable AA NiMH battery (2600 mA h, ~1.2 V) would be able to comfortably power an 8.5 Ohm microheater, consuming 120 mA for about 17 hours and is expected to use 80% of the total battery capacity. A 6-hour incubation was selected to enable detection of 10^6 colony-forming units per mL (CFU mL^{-1}) *E. coli* in one afternoon using the fully charged AA battery and 8 Ohm design A microheater. This higher concentration was used for simplicity of the repeat and is comparable to other publications showing proof-of-concept detection with resazurin.[3] This experiment produced a similarly consistent temperature profile (Fig. 6B) to the DC-powered incubation. Even without adjustable battery power, the microheater maintained an average temperature of 37.4 °C and average estimated sample temperature of 35 °C for the entire 6-hour incubation period.

As seen in Fig. 7A, the 10^6 and 10^4 CFU mL^{-1} (final concentrations 900 CFU μL^{-1} and 9 CFU μL^{-1}) sample pads were all uniformly pink after microheater incubation, indicating reduction of resazurin throughout the sample. In contrast, samples left at room temperature and all negative controls remained visibly dark blue. This proof-of-concept experiment suggests that many other novel designs and heating profiles could be quickly produced using our methods. The quantitative colorimetric analysis shown in Fig. 7B revealed that the microheater incubations produced comparable bacterial growth to the lab-grade incubator results, meanwhile the samples left at room temperature had very little growth. This indicates that the microheaters are able to effectively heat the samples to efficiently grow bacterial samples for culture-based diagnostics. For regions with inconsistent power grids and areas remote from specialized laboratories, portable culture devices could be incubated by these microheaters and could allow for the assessment of food and water quality. These microheaters could be easily combined for existing culture devices, such as those by Deiss *et al.* and Elavarasan *et al.* as

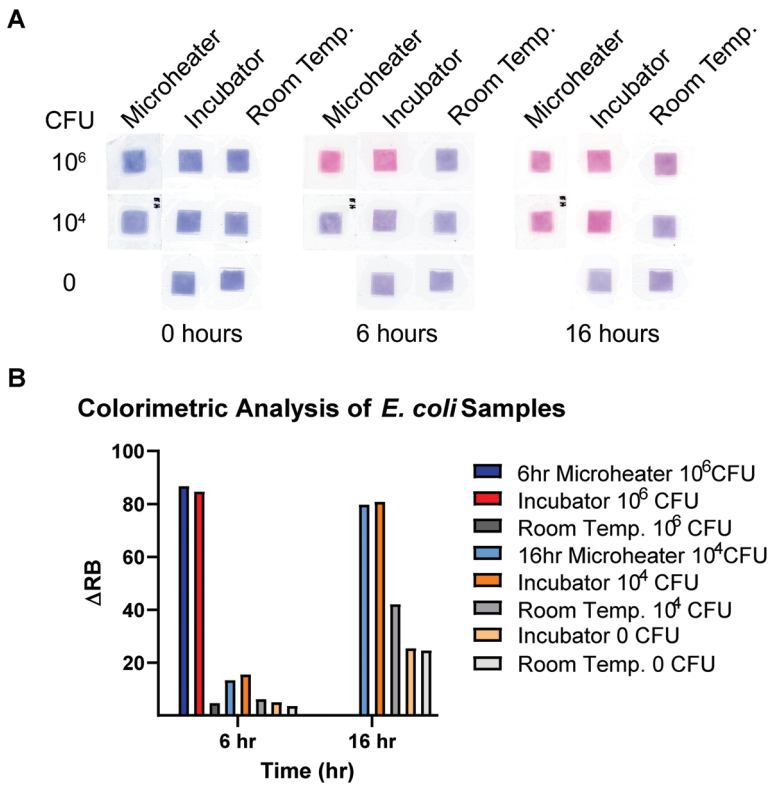

Fig. 7 (A) Colorimetric analysis of the red and blue channel intensities at different time points were summarized into ΔRB values (intensity change from time = 0) to assess the growth of the incubated samples for both the 6- and 16-hour microheater trials. (B) Samples from controls and trials showing intense color change from resazurin reduction. Fig. S9† shows all control concentrations.

well as assessment of antibiotic resistance for the characterization of infectious diseases in these regions.[2,3]

Detection of *V. cholerae via* LAMP amplification. We were able to successfully amplify *V. cholerae* DNA *via* a LAMP assay, indicated by the characteristic positive test band on the LFIAs in Fig. 8A, heated by our microheaters. The test band intensity analysis (Fig. 8B) shows comparable signal between the positive and negative controls heated by the real time machine and the positive and negative samples heated by our microheater. The average temperature of all four incubations (Fig. 8C) was 67 °C (69 °C, 67 °C, 66 °C, 66 °C in order of negative, positive 1, positive 2, and positive 3, respectively) over each 30-minute assay which fell well within our target temperature range of 65–70 °C. The serpentine microheater (design 1_1) in the *V. cholerae* LAMP incubation study had a resistance of 6.4 Ohms and was heated with the same rechargeable NiMH AA battery for all four incubations. The underside of the sample (in contact with the microheater) reached 65 °C within 2–5 minutes of initiation for the first three samples, and above 65 °C within 9 minutes of initiation for the last sample, which had a poor contact and was manually adjusted near the 7-minute mark. After the initial ramp-up time each microheater stayed at or above 65 °C and below 70 °C. LAMP reactions are functional at temperatures as low as 52 °C (ref. 51) but this *V. cholerae* LAMP assay is most efficient and has the fastest amplification rates at a temperature of 65 °C.[52] Despite some poor electrical connections and the same rechargeable NiMH AA battery being used for all 4 experimental incubations, the microheater maintained temperatures within the 65–70 °C incubation window for most of the incubation time.

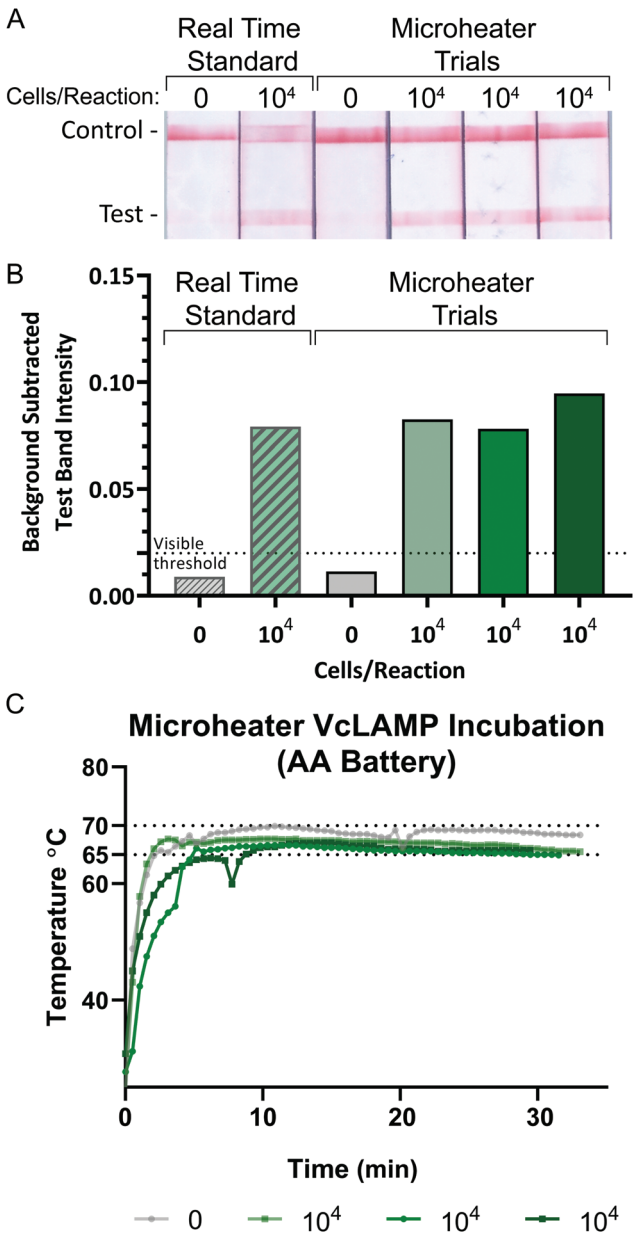

Fig. 8 *V. cholerae* LAMP sample incubation. (A) Commercial LFIAs verifying LAMP amplification of *V. cholerae* DNA from whole cells with positive and negative heating controls amplified in the real-time machine and experimental samples amplified with a 6.4 Ohm microheater (design 1_1). (B) Quantified background subtracted test band intensities of the LFIAs showing comparable visual signal between the heating controls and microheater samples. (C) Temperature profiles of the recorded microheater performance during each ~30-minute incubation.

A cheap, sustainable, and reusable power solution that does not increase waste burdens is critical for increasing accessibility of diagnostics that require heating. Solar powered chargers, while expensive, can be used to charge batteries in remote areas and areas with turbulent power grids to ensure adequate power when necessary. Paper-based batteries have also been investigated and present another alternative for cheap and discreet power for paper devices incorporating printed electronics. One such example is a paper-based battery used for powering an electrochromic display on an electrochemical sensing platform developed by Liu and Crooks.[53] They report an open circuit voltage (OCV) of 1.0 V for their zinc foil and NaCl electrolyte battery which suggests this technology could prove useful for powering microheaters like ours on paper-based assays in the future. Our use of a single rechargeable NiMH AA battery is the lowest power and most sustainable solution for high temperature incubations to-date. Tang *et al.*[54] and Pardy *et al.*[47] both used two AAA alkaline batteries to produce their 3 V potential necessary for heating their LAMP reactions to 65 °C. The Yager lab powered their MAD NAAT assembly containing multiple electronic components including a custom PCB heater with two AA batteries. Pardy *et al*. discussed the positive attributes of alkaline batteries including their low price, relatively small size and good energy density, however NiMH batteries also have these qualities and are known to provide a better voltage plateau (meaning more stable discharge over time) than rechargeable alkaline batteries resulting in more consistent heating for a longer time period.[47,48] Alkaline and NiMH batteries are both considered non-hazardous waste and can be recycled if recycling is available in the region. By reducing the power by more than half (from 3 V to 1.2 V), we also enable a greater ability to incorporate these microheaters into cheap and portable cell phone powered platforms for multi-temperature and sequential

heating, which was successful.[55] We hope this work can be built upon using our simple methods to further the potential for accessible diagnostics worldwide.

Conclusions

We have fabricated, characterized, modeled, and demonstrated the use of low-power printed nanosilver ink microheaters in proof-of-concept experiments supporting low-power in-field and POC diagnostic applications. The microheaters are reusable, wettable, durable to bending, and can be used to precisely heat discrete regions to 37 °C or 65 °C within three minutes and held at temperature for up to 16 hours and 30 minutes, respectively. Consistent performance with minimal insulation was demonstrated. These microheaters can be used for automated, rapid, and sustained heating of microfluidic samples and paper components. The thermal properties emerging from the design of these microheaters can be quickly modified for specific geometries and incorporation into scalable roll-to-roll device manufacturing. We demonstrated diverse thermal incubation reactions using a single NiMH AA rechargeable battery for four consecutive 30-minute LAMP assays and a bacterial detection test incubated for 6 hours with two different microheater designs respectively. These inkjet-printed microheaters can be customized for heating in sample preparation, amplification or incubation, and detection processes in increasingly intricate paper and multi-material devices. The printing method allows for easy testing of new designs for any heating region size or shape. These methods resulted in a set of microheaters that are reusable, can be wetted, are durable to bending, do not physically degrade or deform upon heating, provide even heating without hotspots, and maintain a stable resistance over 6 months.

Further investigation and standardization of drop-spacing and other print settings can decrease variability of printed traces and give rise to industry scalable roll-to-roll settings and solidify the true potential of these techniques to heat small reactions while using minimal power. Because of their low power requirements, these microheaters can be easily integrated into emerging sample-to-answer nucleic acid amplification platforms powered by a simple battery or regulated by a microUSB connected to a lithium ion battery or smartphone.

Conflicts of interest

There are no conflicts of interest for this project.

Acknowledgements

This project was funded in part by the Bill and Melinda Gates Grand Challenges Explorations program grant OPP1150806, and Purdue University Shaw Global Innovation Laboratory's Innovations in International Development Award, and a Ross Fellowship from the Weldon School of Biomedical Engineering. We would like to thank Nicholas Glassmaker at the Purdue University Birck Nanotechnology Center for assisting with the profilometry data acquisition.

References

1 G. Otsuka and T. Nakae, *J. Dairy Sci.*, 1969, **52**, 2041–2044.
2 T. Elavarasan, S. K. Chhina, M. Parameswaran (Ash) and K. Sankaran, *Sens. Actuators, B*, 2013, **176**, 174–180.
3 F. Deiss, M. E. Funes-Huacca, J. Bal, K. F. Tjhung and R. Derda, *Lab Chip*, 2014, **14**, 167–171.
4 B. J. Toley, I. Covelli, Y. Belousov, S. Ramachandran, E. Kline, N. Scarr, N. Vermeulen, W. Mahoney, B. R. Lutz and P. Yager, *Analyst*, 2015, **140**, 7540.
5 T. Notomi, *Nucleic Acids Res.*, 2000, **28**, 63e.
6 J. Cook, B. Aydin-Schmidt, I. J. González, D. Bell, E. Edlund, M. H. Nassor, M. Msellem, A. Ali, A. K. Abass, A. Mårtensson and A. Björkman, *Malar. J.*, 2015, **14**, 43.
7 L. K. Lafleur, J. D. Bishop, E. K. Heiniger, R. P. Gallagher, M. D. Wheeler, P. Kauffman, X. Zhang, E. C. Kline, J. R. Buser, S. Kumar, S. A. Byrnes, N. M. J. Vermeulen, N. K. Scarr, Y. Belousov, W. Mahoney, B. J. Toley, P. D. Ladd, B. R. Lutz and P. Yager, *Lab Chip*, 2016, **16**, 3777–3787.
8 X. Jiang, J. C. Loeb, C. Manzanas, J. A. Lednicky and Z. H. Fan, *Angew. Chem., Int. Ed.*, 2018, **57**, 17211–17214.
9 J. Song, M. G. Mauk, B. A. Hackett, S. Cherry, H. H. Bau and C. Liu, *Anal. Chem.*, 2016, **88**, 7289–7294.
10 M. Sema, A. Alemu, A. G. Bayih, S. Getie, G. Getnet, D. Guelig, R. Burton, P. LaBarre and D. R. Pillai, *Malar. J.*, 2015, **14**, 44.
11 J. C. Linnes, A. Fan, N. M. Rodriguez, B. Lemieux, H. Kong and C. M. Klapperich, *RSC Adv.*, 2014, **4**, 42245–42251.
12 M. Packard, E. Wheeler, E. Alocilja and M. Shusteff, *Diagnostics*, 2013, **3**, 105–116.
13 E. A. Phillips, R. Shen, S. Zhao and J. C. Linnes, *Lab Chip*, 2016, **16**, 4230–4236.
14 S. Byrnes, G. Thiessen and E. Fu, *Bioanalysis*, 2013, **5**, 2821–2836.
15 Southwest Science Incubators, http://www.southwestscience.com/Incubators.html, (accessed 2 March 2019).
16 T. Pardy, T. Rang and I. Tulp, *Micromachines*, 2017, **8**, 180.
17 S. Huang, J. Do, M. Mahalanabis, A. Fan, L. Zhao, L. Jepeal, S. K. Singh and C. M. Klapperich, *PLoS One*, 2013, **8**, e60059.
18 K. G. Shah, D. Guelig, S. Diesburg, J. Buser, R. Burton, P. LaBarre, R. Richards-Kortum and B. Weigl, *PLoS One*, 2015, **10**, e0139449.
19 J.-T. Wu, S. Lien-Chung Hsu, M.-H. Tsai, Y.-F. Liu and W.-S. Hwang, *J. Mater. Chem.*, 2012, **22**, 15599.
20 D. Gosselin, D. Chaussy, N. Belgacem, F. Navarro and J. Berthier, *Transducers Heat Transfer Correlations for Free Convection from Suspended Microheaters, Toronto*, 2016, vol. 203.
21 A. C. Siegel, S. T. Phillips, B. J. Wiley and G. M. Whitesides, *Lab Chip*, 2009, **9**, 2775–2781.

22 A. Botau, D. Bonfert, C. Negrea, P. Svasta and C. Ionescu, in 2015 38th International Spring Seminar on Electronics Technology (ISSE), IEEE, 2015, pp. 358–363.
23 J. Park, K. Shin and C. Lee, *Int. J. Precis. Eng. Manuf.*, 2016, **17**, 537–550.
24 J. Perelaer and U. S. Schubert, *J. Mater. Res.*, 2013, **28**, 564–573.
25 S.-H. Park, S.-M. Lee, E.-H. Ko, T.-H. Kim, Y.-C. Nah, S.-J. Lee, J. H. Lee and H.-K. Kim, *Sci. Rep.*, 2016, **6**, 33868.
26 P.-H. Wang, S.-P. Chen, C.-H. Su and Y.-C. Liao, *RSC Adv.*, 2015, **5**, 98412–98418.
27 M. Hummelgård, R. Zhang, H.-E. Nilsson and H. Olin, *PLoS One*, 2011, **6**, e17209.
28 W. Shen, X. Zhang, Q. Huang, Q. Xu and W. Song, *Nanoscale*, 2014, **6**, 1622–1628.
29 S. H. Ko, H. Pan, D. J. Hwang, J. Chung, S. Ryu, C. P. Grigoropoulos and D. Poulikakos, *J. Appl. Phys.*, 2007, **102**, 093102.
30 J. S. Kang, J. Ryu, H. S. Kim and H. T. Hahn, *J. Electron. Mater.*, 2011, **40**, 2268–2277.
31 C. Silveira, T. Monteiro and M. Almeida, *Biosensors*, 2016, **6**, 51.
32 S. F. Jahn, T. Blaudeck, R. R. Baumann, A. Jakob, P. Ecorchard, T. Rüffer, H. Lang and P. Schmidt, *Chem. Mater.*, 2010, **22**, 3067–3071.
33 R. Worsley, L. Pimpolari, D. McManus, N. Ge, R. Ionescu, J. A. Wittkopf, A. Alieva, G. Basso, M. Macucci, G. Iannaccone, K. S. Novoselov, H. Holder, G. Fiori and C. Casiraghi, *ACS Nano*, 2019, **13**, 54–60.
34 S. Bae, H. Kim, Y. Lee, X. Xu, J.-S. Park, Y. Zheng, J. Balakrishnan, T. Lei, H. Ri Kim, Y. Il Song, Y.-J. Kim, K. S. Kim, B. Özyilmaz, J.-H. Ahn, B. H. Hong and S. Iijima, *Nat. Nanotechnol.*, 2010, **5**, 574–578.
35 M. J. Cordill, O. Glushko, J. Kreith, V. M. Marx and C. Kirchlechner, *Microelectron. Eng.*, 2015, **137**, 96–100.
36 C. A. Holstein, *Development of a Novel Paper-Based Flu Test for Improved Diagnosis at the Point of Care*, PhD Dissertation, University of Washington, 2015.
37 NEB Inc., Can Bst 2.0 DNA Polymerase be used at temperatures other than 65 °C? | NEB, https://www.neb.com/faqs/2012/08/28/can-bst-2-0-dna-polymerase-be-used-at-temperatures-other-than-65-c, (accessed 11 July 2019).
38 D. A. Roberson, R. B. Wicker, L. E. Murr, K. Church, E. MacDonald, D. A. Roberson, R. B. Wicker, L. E. Murr, K. Church and E. MacDonald, *Materials*, 2011, **4**, 963–979.
39 B. Derby, *Annu. Rev. Mater. Res.*, 2010, **40**, 395–414.
40 S. Jung, A. Sou, E. Gili and H. Sirringhaus, *Org. Electron. physics, Mater. Appl.*, 2013, **14**, 699–702.
41 NovaCentrix, 2015.
42 R. F. Saraf, J. M. Roldan, R. Jagannathan, C. Sambucetti, J. Marino and C. Jahnes, in 1995 Proceedings. 45th Electronic Components and Technology Conference, IEEE, pp. 1051–1053.
43 J. Wang, H. L. Duan, Z. P. Huang and B. L. Karihaloo, *Proc. R. Soc. London, Ser. A*, 2006, **462**, 1355–1363.
44 M. Cao, K. Jochem, W. J. Hyun, L. F. Francis and C. D. Frisbie, *Flexible Printed Electron.*, 2018, **3**, 045003.
45 H. A. D. Nguyen, K. Shin and C. Lee, *Int. J. Precis. Eng. Manuf.*, 2015, **16**, 517–523.
46 D. Kapton®, *DUPONT ™ KAPTON ® HN POLYIMIDE FILM*.
47 T. Pardy, I. Tulp, C. Kremer, T. Rang and R. Stewart, *PLoS One*, 2017, **12**, e0189968.
48 Energizer, *Nickel Metal Hydride (NiMH) Handbook and Application Manual*, 2010.
49 B. Sadri, D. Goswami, R. Martinez, B. Sadri, D. Goswami and R. V. Martinez, *Micromachines*, 2018, **9**, 420.
50 L. P. Candeias, D. P. S. Macfarlane, S. L. W. Mcwhinnie, N. L. Maidwell, C. A. Roeschlaub, P. G. Sammes and R. Whittlesey, *The catalysed NADH reduction of resazurin to resorufin*, 1998.
51 M. S. Yoo, J. H. Noh, B. S. Yoon, K. E. Reddy, C. H. Kweon, S. C. Jung and S. W. Kang, *J. Virol. Methods*, 2012, **186**, 147–151.
52 J. C. Rolando, E. Jue, N. G. Schoepp and R. F. Ismagilov, *Anal. Chem.*, 2019, **91**, 1034–1042.
53 H. Liu and R. M. Crooks, *Anal. Chem.*, 2012, **84**, 2528–2532.
54 R. Tang, H. Yang, Y. Gong, M. L. You, Z. Liu, J. R. Choi, T. Wen, Z. Qu, Q. Mei and F. Xu, *Lab Chip*, 2017, **17**, 1270–1279.
55 E. A. Phillips, T. J. Moehling, K. F. K. Ejendal, O. S. Hoilett, K. M. Byers, L. A. Basing, L. A. Jankowski, J. B. Bennett, L.-K. Lin, L. A. Stanciu and J. C. Linnes, *Lab Chip*, 2019, **19**, 3375–3386.